

## **C. Instrumentation for electrical bioimpedance measurements**

The objective of this section is to describe the main issues concerning the developed instrumentation for electrical impedance measurements. It focuses on the particular aspects of the instrumentation that are more related with the application and leaves out the details about those issues that can be considered more general in the electronic instrumentation field.

Although not many, there exist some interesting general documents related to electrical impedance measurement systems [1-3]

### C.1. General issues concerning the developed instrumentation

As for any kind of instrumentation system, the appropriate general architecture of an impedance analyzer largely depends on the frequencies of interest. In this sense it must be mentioned that the frequency range of all the developed systems goes from 10 Hz to 1 MHz.

Conceptually, the developed impedance measurement systems can be split into two sub-systems (Figure C. 1):

- The gain/phase analyzer. It is responsible to generate a reference sinusoidal voltage or current, to obtain the in-phase and in-quadrature components of the incoming voltages or currents and to compute and display the resulting values.
- The signal conditioning sub-system. It is responsible to adapt the inputs and outputs of the gain/phase analyzer in order to perform the electrical bioimpedance measurement. It basically includes some voltage-to-current or current-to-voltage converters and a differential amplifier.

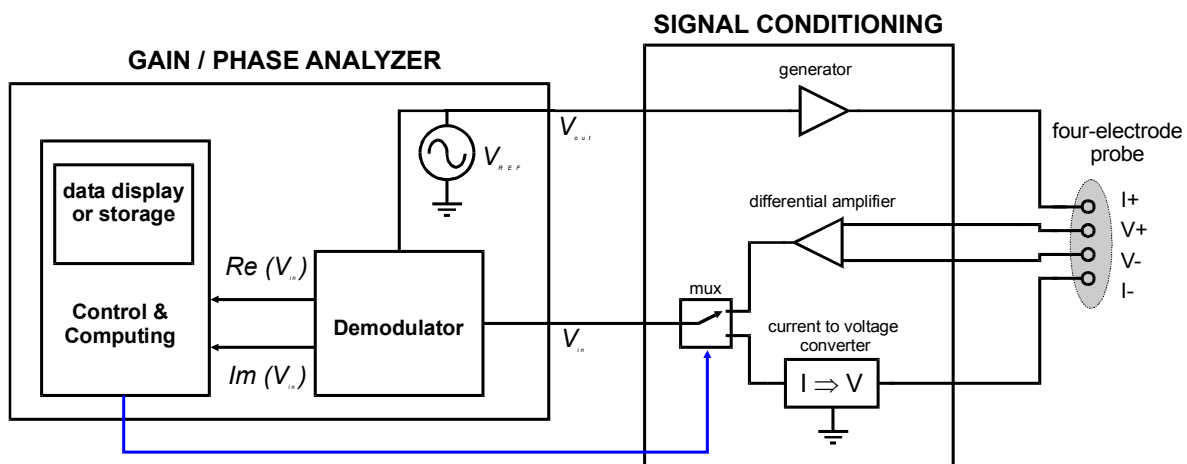


Figure C. 1. Conceptual implementation of bioimpedance measurement systems.

#### C.1.1. The gain/phase analyzer

This system is not exclusive of impedance analyzers, it can be also employed, for instance, to study the response of filters. It generates a sinusoidal signal, typically a voltage, and demodulates the incoming signal according to the frequency and phase of the reference signal to obtain the in-phase and the in-quadrature signal amplitudes, which are equivalent to real part and the imaginary part of the signal.

## Sinusoidal signal generation

Different methods can be applied to generate the reference sinusoidal signal:

- Sinusoidal oscillator

There are some well known analog schemes, such as the Wien-bridge oscillator [4], able to generate sine signals. However, these schemes require an accurate matching of some resistance and capacitance values that constrain their applicability. As a consequence, they are becoming obsolete in most applications in favor of digitally based techniques.

- Sine converter

By using the nonlinear features of diodes and transistors, it is possible to implement arbitrary nonlinear functions able to shape triangular waves [4]. This fact is used by some integrated waveform generators, such as the XR-8038A (Exar Corp., CA, USA), to obtain sine waves from triangular waves which in turn are obtained from rectangular waves generated by stable oscillators.

Such sine generators are frequency programmable and provide the necessary in-quadrature reference signal. However, the distortion of the sinusoidal signal and, particularly, their power consumption limit their usage.

- Sinusoid from rectangular pulses by Low Pass Filtering

This is a very effective, economic and simple way to obtain the sinusoidal signals. A simple digital circuit, or a simple algorithm embedded in a microcontroller, can provide the necessary reference square wave and the in-quadrature signal (delayed  $T/4$ ). The filter order will depend on the application, even a second-order filter could be enough in some cases [5].

The main drawback of this technique is that the frequency cannot be changed if the filter is not modified. It is possible to think of some strategies to modify the cutoff frequency by using programmable filters or switched-capacitor methods. However, in this case the added complexity is so high that currently it makes more sense to employ Direct Digital Synthesis.

- Direct Digital Synthesis (DDS)

DDS is a digital technique for generating an output waveform (sine, square or triangular) or clocking signal from a fixed frequency clock source. Its basic structure is depicted in Figure C. 2. The signal is digitally generated, by means of a hardware scheme such as that shown in Figure C. 2 or through a software approach, and converted to its equivalent analog signal by an Digital to Analog Converter (DAC). The Low Pass Filter smoothes the output signal from the DAC and, in this way, minimizes the high-frequency harmonics.

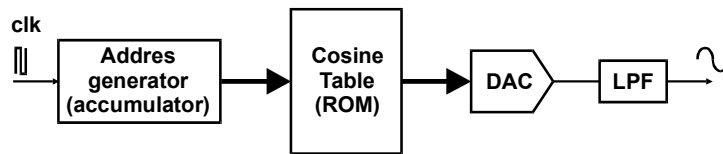


Figure C. 2. Direct Digital Synthesis.

Currently, DDS is probably the optimum choice for sine generation in terms of costs, power consumption and space, particularly in multi-frequency systems. There exist some commercial integrated circuits that implement this function up to some hundred of MHz (<http://www.analog.com>).

Whatever the sine generation method is, it must be taken into account that it is desirable to obtain a signal in-quadrature with the reference signal for the demodulation process. That is, a signal delayed  $T/4$  or with a phase shift of 90 degrees with respect to the reference signal. This is very simple in the case of digital schemes. In the case of analog schemes it is possible to employ phase shifters but the  $T/4$  shift will only be obtained for a single frequency.

## Demodulation

An intuitive idea of how to measure the amplitude and the phase of a signal is to use a peak detector for the amplitude and a phase detector, for instance, based on zero crossings [6], for the phase. However, this is not a good approach in the case of bioimpedance since the injected current is very low and the environment is quite noisy (the sample can generate voltages by itself). Thus, it is advisable to use some kind of demodulation to reject the noise or the interferences that are not in the frequency range of interest. Generally, the bioimpedance changes are very slow and this implies that the frequency range of interest has a spectral width of some Hz and is centered on the frequency of the reference signal. Because of such signal features, coherent demodulation, also called synchronous demodulation or detection, is employed in most cases:

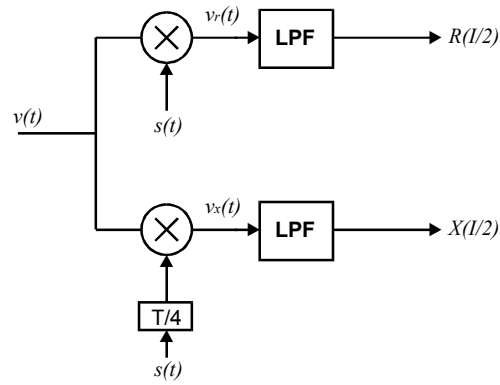


**Figure C. 3.** Coherent demodulation.

Mathematical formulation of the coherent demodulation scheme and its performance concerning noise rejection is presented elsewhere [7;8], however, for the reader convenience here it is briefly introduced:

Consider that, in Figure C. 3,  $s(t)=\cos(2\pi f_0 t)$  represents the reference signal, that the impedance at frequency  $f_0$  is constant  $Z = |Z| \cos(\theta) + j \cdot |Z| \sin(\theta) = R + jX$  (resistance and reactance) and that it is measured by the injection of the current  $i(t)=I \cdot s(t)$ ,

$$v(t) = z i(t) = I|Z| \cos(2\pi f_0 t + \theta) \quad (\text{C.1})$$

then, the signal at the upper branch before the Low Pass Filter is:

$$v_r(t) = I|Z| \cos(2\pi f_0 t + \theta) \cdot \cos(2\pi f_0 t) \quad (\text{C.2})$$

$$v_r(t) = I|Z| [\cos(2\pi f_0 t) \cdot \cos(2\pi f_0 t) \cdot \cos(\theta) + \sin(2\pi f_0 t) \cdot \cos(2\pi f_0 t) \cdot \sin(\theta)] \quad (\text{C.3})$$

$$v_r(t) = I|Z| \left[ \frac{\cos(2\pi 2f_0 t) \cdot \cos(\theta)}{2} + \frac{\cos(\theta)}{2} + \frac{\sin(2\pi 2f_0 t) \cdot \sin(\theta)}{2} \right] \quad (\text{C.4})$$

Since the LPF is designed to reject components above the bioimpedance signal frequency width ( $\ll f_0$ ), at the output of the upper branch we have  $I|Z| \cos(\theta)/2$  which is equivalent to  $R(I/2)$ .

For the lower branch:

$$v_x(t) = I|Z| \cos(2\pi f_0 t + \theta) \cdot (-\sin(2\pi f_0 t)) \quad (\text{C.5})$$

and it is obtained that at the output we have  $I|Z| \sin(\theta)/2$  which is equivalent to  $X(I/2)$ . Therefore, coherent demodulation can be employed to obtain the resistance and the reactance of an impedance at a certain frequency.

Coherent demodulation can be implemented in different ways. For high frequencies ( $>10$  MHz), analog mixers (i.e. multipliers) are employed in a scheme totally equivalent to that of Figure C. 3. However, for lower frequencies other structures are preferred to avoid the use of mixers. Two of those alternative structures have been tried in the developed systems<sup>1</sup>:

- Synchronous demodulation based on sign switching

In the case that  $v(t)$  is multiplied by a zero mean square signal with the same frequency and phase of  $s(t)$ ,  $R$  and  $X$  can be obtained with the same scheme since the replicas caused by the high frequency harmonics of the square signal are also filtered by the LPF (details are provided elsewhere [10]).

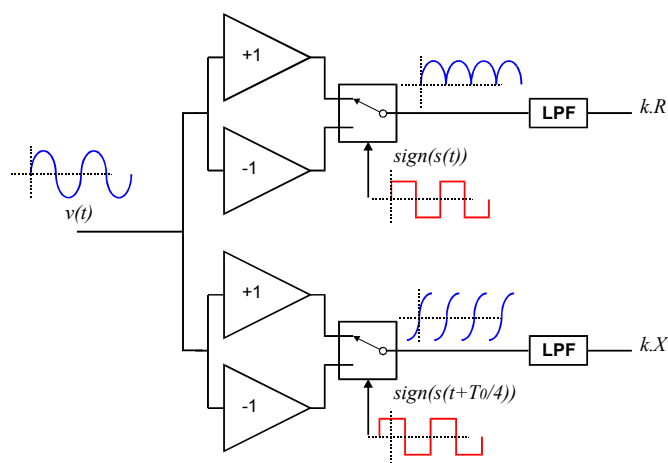


Figure C. 4. Synchronous demodulation based on sign switching.

There exist some integrated circuits that develop this function such as AD630 (Analog Devices). Although the frequency bandwidth of the amplifiers can be more than enough for many applications ( $> 1$  MHz), the features of the analogue switches usually limit the useful bandwidth of the overall system at much lower frequency. Currently, by implementing the structure with enhanced external switches it is possible to get working bandwidths up to some hundreds of kHz.

- Digital demodulation

It is possible to perform the demodulation process in a completely digital way by implementing the digital equivalent of the structure depicted in Figure C. 3.

<sup>1</sup> It must be noted that another demodulation method, half-way between analog switching and digital demodulation, has been developed by Pallás-Areny and Webster for bioimpedance measurements [9].

The following figures and equations try to show how it is possible to obtain R and X in a digital manner. In this example it has been chosen to perform 8 samples per period but any other value could be possible, even one sample per period, the only requisite is to be able to take two sub-sets of samples delayed  $T_0/4$ .

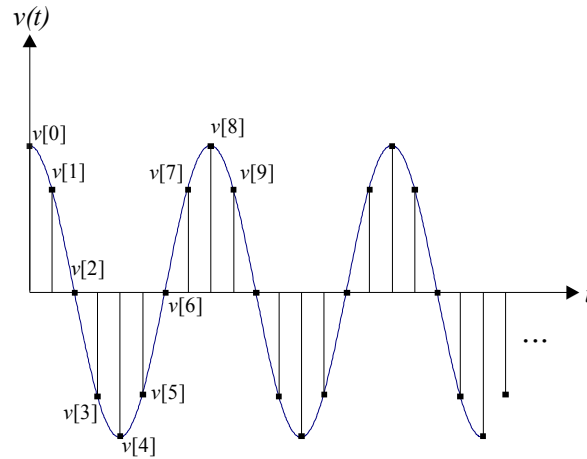


**Figure C. 5.** Sampling an analog signal in the case  $T_{ACQ} \ll T_0$ .

In the case that the  $T_{ACQ}$  is larger than  $T_0/8$  it is possible to take the sample  $n+1$  in the next period, it is even possible to ignore as many periods as necessary. That is the 'undersampling' concept [11;12]. .

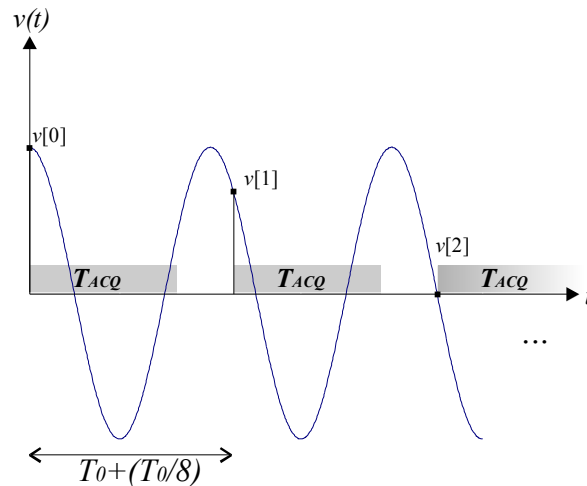


**Figure C. 6.** Sampling in the case  $T_{ACQ} > T_0/8$ .

The resistance component (R) will be obtained by filtering with a digital LPF the signal:

$$v_r[n] = v[n] \cos[2\pi(n/8)] \quad (C.6)$$

and the reactive component (X) will be obtained by filtering the signal:

$$v_x[n] = v[n-2]\cos[2\pi(n/8)] \quad (\text{C.7})$$

That is, the two samples delay is equivalent to  $T_0/4$ .

In principle, digital demodulation does not imply the use of high sampling rate ADCs since undersampling techniques can be applied. That is, it is not necessary to employ ADCs with sampling frequencies above  $2f_0$ . However, the aperture time of the ADC is a critical parameter that is usually specified in accordance to the ADC sampling rate and, at the end, ADCs with high sampling rates are required.

A constant aperture delay of the ADC affects in the same manner to the resistance and reactance components and causes a constant phase error that can be canceled by calibration. However, the aperture jitter, due to the clock jitter or to ADC sample-and-hold jitter, will cause a random error that can be regarded as noise. This source of error will affect seriously to the phase measurement. For instance, Figure C. 7 shows the standard deviation of the phase angle that the results from a Matlab simulation of the measurement of a 100 kHz signal when the jitter rangers from 1 ns to 100 ns.

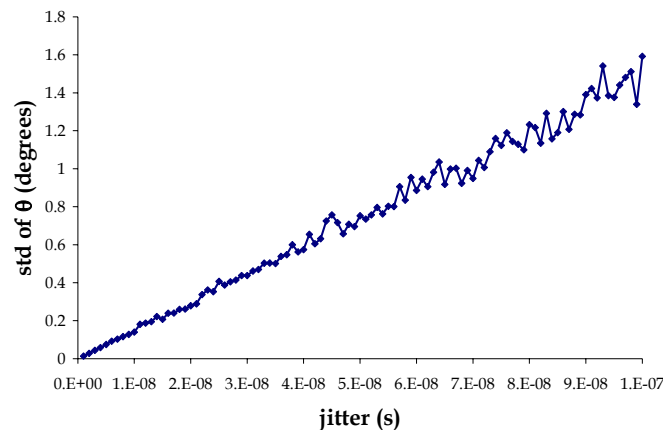


**Figure C. 7.** Simulated standard deviation of the phase angle measurement vs. the ADC jitter time in the case that  $f_0 = 100$  kHz and the R and X values are obtained by averaging 8 samples.

It must be mentioned that in the case that the system response is linear, in principle, it is also possible to obtain the impedance at any frequency by injecting other signals than sinusoids, for instance, rectangular pulses. This can be achieved by performing the Fourier transform to the obtained time response after applying the pulse. Such strategy has been used by some authors in the bioimpedance field [13-15] and it can be beneficial in terms of measurement time.



### C.1.2. The signal-conditioning electronics

The developed systems are based on the so called auto balancing bridge method (Figure C. 1). The current flowing through the impedance sample ( $Z_x$ ) also flows through the resistor  $R$ . The voltage at the '0' node is maintained at zero volts ('virtual ground') because the current through  $R$  balances with the sample current by operation of the I-V converter amplifier, also called transimpedance amplifier. In this way, the impedance is computed from the voltage difference at the sample and the voltage output of the transimpedance amplifier which is proportional to the current flowing through the sample.

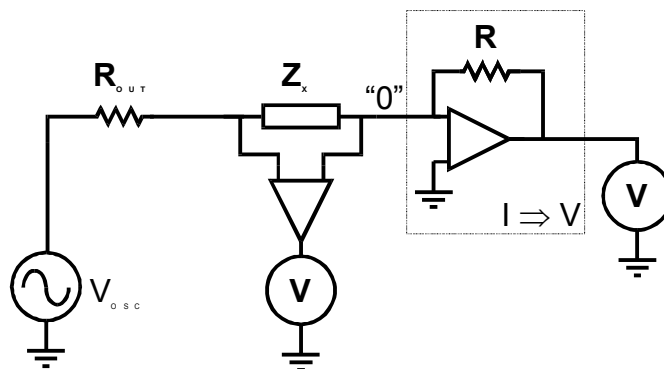


**Figure C. 8.** Schematic representation of the auto balancing bridge method. Note that the electrode impedances are not represented.

This measurement method has been previously used in the bioimpedance field for frequency ranges up to some MHz [11;16].

It must be noted that at the beginning we tried a measurement method in which the current injected to the sample was fixed by a feedback strategy (Figure C. 9). However, such method is not only prone to instability but it also implies a serious drawback concerning safety: when the instrumentation is not connected to the sample, the amplifier output is saturated at a voltage close to that of the supply unless a voltage clamping method is included and, when it becomes connected to the sample, a transitory period occurs before the injected current reaches the desired level, thus, dangerous current levels and wave shapes can be injected to the sample<sup>2</sup>. Moreover, the reference resistance  $R$  must be sufficiently small to avoid significant common voltage.

<sup>2</sup> Other constant current methods are possible [17-19], however, the dangerous phenomenon related to the connection and disconnection of the sample is not avoided.

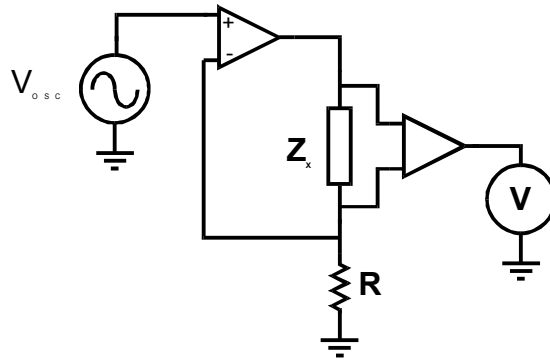


**Figure C. 9.** Feedback control of the current flowing through the sample. This method is not recommended (see the text).

### The output resistance ( $R_{OUT}$ )

If  $R_{OUT} \rightarrow \infty$ , the output voltage source is equivalent to a current source and the transimpedance amplifier is not necessary since the current does not depend on the load. Unfortunately, that situation would imply a infinitesimal voltage difference at the sample under test. Hence, a limited value resistance is required and some sort of current dependence on the load will exist<sup>3</sup>.

Nevertheless, the actual purpose of  $R_{OUT}$  is to limit the maximum current flowing through the sample under any circumstance, including transitory regimes, malfunction or failure of any component related with the generator. For instance, a  $1\text{ M}\Omega$  resistor in a circuit powered by  $\pm 5\text{ V}$  guarantees that the maximum current amplitude will be  $5\ \mu\text{A}$  which is a very safe value for any frequency and for any living tissue.

### The current-to-voltage converter

This subsystem can be implemented as it is shown in Figure C. 10 with a standard operational amplifier. Negative feedback brings the input voltage to zero (zero input impedance), all the injected current flows through  $R_f$  and  $V_{OUT} = -R_f \cdot I$  (the gain can be expressed in  $\Omega$  and for that reason these structures are also referred as transimpedance amplifiers). Unfortunately, the stray capacitance ( $C_s$ ) combined with  $R_f$  creates an undesired pole within the gain bandwidth of the op-amp that can induce instability. To avoid problems caused by such pole, a feedback capacitance ( $C_f$ ) is included that reduces the bandwidth of the current-to-voltage converter [20].

<sup>3</sup> In some applications the current error is not significant and the transimpedance amplifier can be avoided.

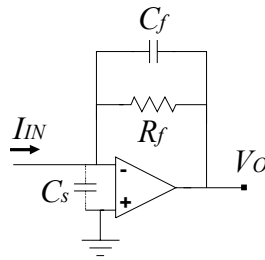


**Figure C. 10.** Current-to-voltage converter based on a voltage feedback operational amplifier.

A better solution is to use a current-feedback op-amp (CFA) instead of a voltage-feedback op-amp [21]. In this way, the pole caused by the stray capacitance ( $C_s$ ) is determined by the input resistance which is a low value resistance ( $\sim 50 \Omega$ ). Therefore, the pole appears at such a high frequency that it does not cause stability problems<sup>4</sup>.

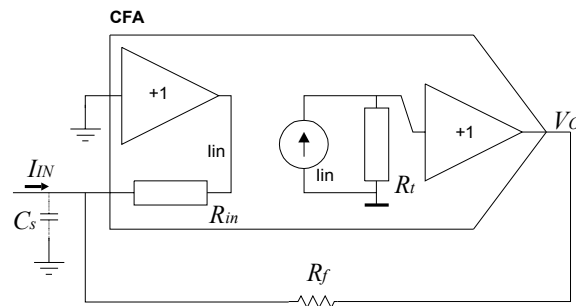


**Figure C. 11.** Current-to-voltage converter based on a current-feedback amplifier.

The input of the transimpedance amplifier can be a weak point concerning safety in the case of failure. Resistances and capacitances could be added to limit current levels but that would lessen the performance of the overall system. Voltage clamping diodes will improve the safety but are not definitive solution. Fortunately, in the case that the system is electrically isolated (i.e. floating) from other instruments electrically connected to the sample, the protection mechanisms at the output of the oscillator ( $R_{OUT}$ ) and at the differential amplifier inputs avoid any possibility of current flowing through the sample from the transimpedance amplifier.

### The differential amplifier

A more detailed representation of the auto balancing scheme including the electrode impedances will be useful to illustrate the main issues concerning the differential amplifier stage.

<sup>4</sup> In this case, to include a feedback capacitance is not a good idea at all, it could cause instability.

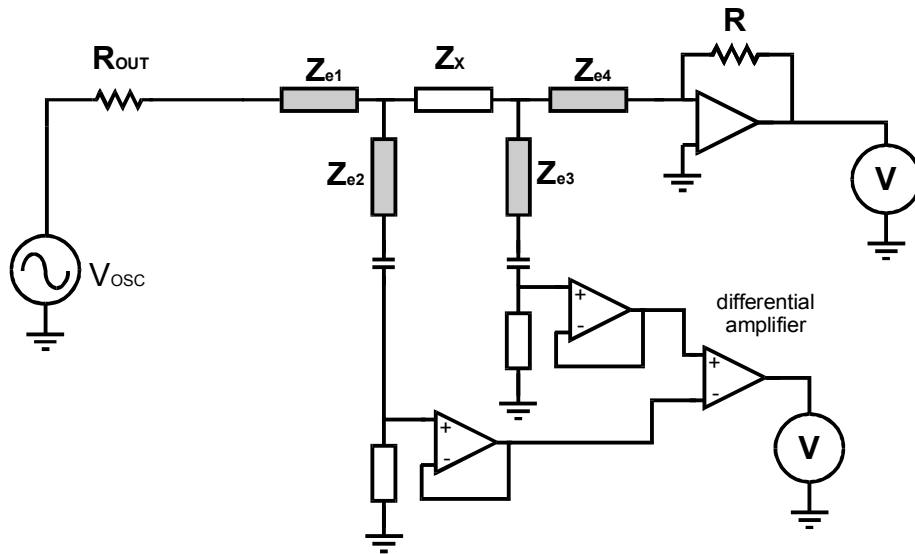


**Figure C. 12.** Representation of the auto-balancing bridge method including the electrode impedances and a detailed possible implementation of the differential amplifier.

The impedance of the I- electrode ( $Z_{e4}$ ) causes a common voltage that must be rejected by the differential amplifier thanks to its high CMRR. As it has been mentioned in chapter 2, the effective CMRR will largely depend on the input impedances seen from the voltage electrodes  $V+$  and  $V-$  [22]. It is desirable to get those impedances as high and matched as possible. Therefore, two important features of the differential amplifier must be: high intrinsic CMRR over the frequency band of interest and high input impedances.

Of course, the gain bandwidth is also an important feature but, taken into account the frequency band of interest in the framework of this thesis work (up to 1 MHz), it should not be an issue here. Moreover, the phase error at high frequencies can be easily compensated by a calibration procedure.

Instrumentation amplifiers usually have very high CMRR figures at DC or low frequencies but their behavior is poor at high frequencies (>10 kHz). It is more convenient to employ what the manufacturers usually refer as 'differential amplifiers'. Those integrated circuits are typically optimized for communications and, since low output impedance sources are assumed in such applications, their input impedance features are not suitable for bioimpedance measurements. Thus, it is advisable to include high input impedance buffers between the electrodes and the differential amplifier to achieve a high effective CMRR. Those buffers can be implemented with operational amplifiers configured as voltage followers.

If capacitors are included at the buffers inputs to avoid any chance of DC current flowing through the sample, polarization resistances will be necessary. In this case,

low input bias current OAs will be the choice to allow the use of very high polarization impedances and avoid a decrease of the effective CMRR.

### Isolation

Galvanic isolation of bioimpedance instrumentation with respect to the mains supply and the earth ground is not only a safety requirement [23] but also an advisable feature for accuracy<sup>5</sup>. In the case that the sample is somehow connected to the earth ground, the instrumentation must be isolated in order to avoid leakage currents from the impedance probe that would surely distort the impedance measurements. Moreover, if there are other instruments connected to the sample, these instruments must be also isolated with respect to the impedance meter to avoid the same phenomenon.

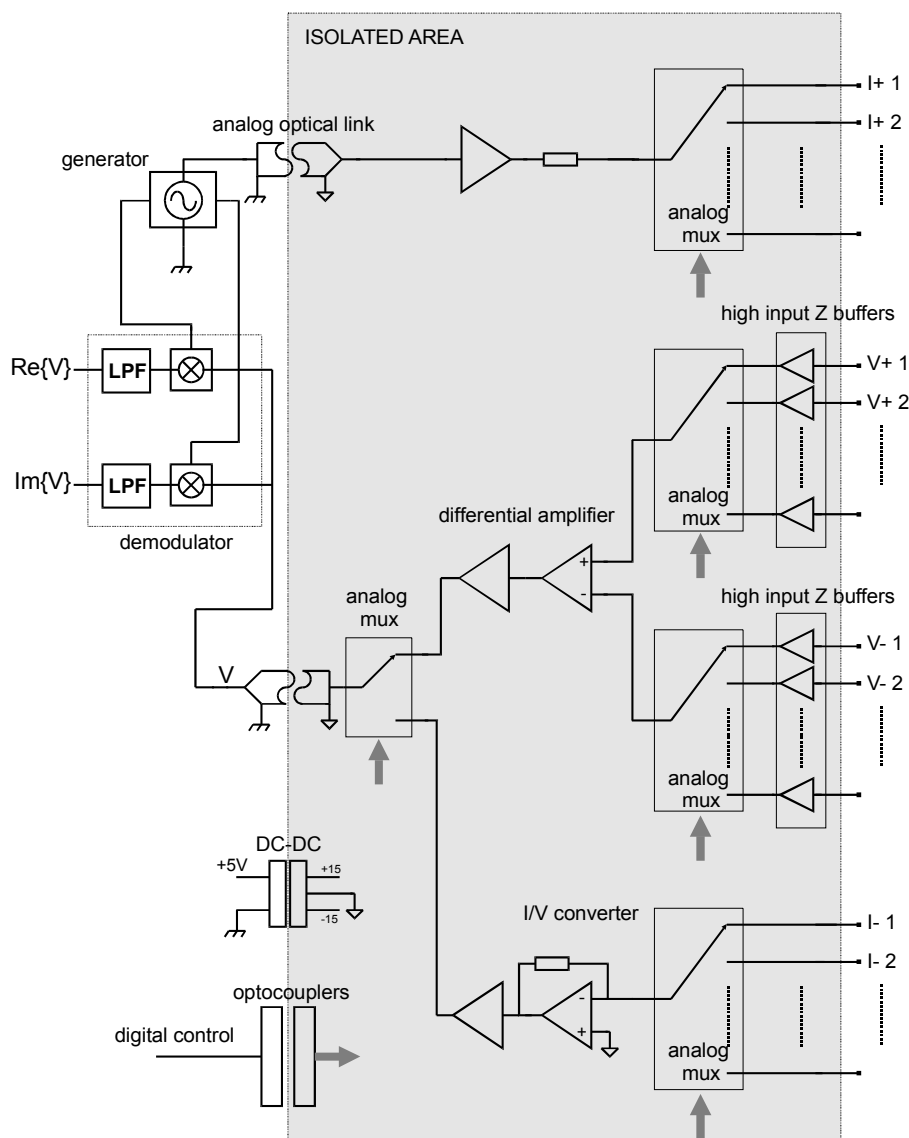


Figure C. 13. Implementation example of an isolated front-end.

<sup>5</sup> Isolation can also be employed to avoid the effect of stray capacitances of electrodes leads [17].

Of course, it is not necessary to isolate the whole instrument, it is just necessary to isolate the sample leads. That implies that the isolation barrier can be placed at any convenient position between the mains and the leads. For instance, the isolation barrier can be placed between the signal conditioning electronics and the gain/phase analyzer.

It must be taken into account that isolation transformers optimized for medical equipment or isolated DC-DC converters can have a very high isolation impedance at 50 Hz but, as frequency increases, such impedance is reduced and can cause problems at frequencies higher than 100 kHz. For instance, an typical coupling capacitance of 100 pF in an isolation transformer means  $\sim 30 \text{ M}\Omega$  at 50 Hz but only  $1600 \Omega$  at 1 MHz.

Needles to say that battery powered sub-systems with optical (e.g. optocouplers or optic fiber) or radiofrequency communications with the main instrument are a perfect solution for isolation.

### Guards and shields

As it has been mentioned in chapter 2, the parasitic impedances between the instrumentation terminals lessen the system's overall performance, particularly at high frequencies. It is evident that the parasitic capacitances of the wires that connect the electrodes to the instrumentation make worse the situation. Thus, it is advisable to minimize the cable length, to minimize the parasitic impedance per length (for instance, separating the wires) and to use some strategies that compensate or cancel the effect of such parasitic capacitances. One of such strategies is to use shielded wires<sup>6</sup> combined with active electronics in order to create active guards [10]. The key idea of active guarding is to drive the shield at the same voltage than the signal (core) to avoid any chance of current leakage from the signal wire. In this way the effective input capacitance is minimized and the interference rejection given by the shield is maintained (Figure C. 14).

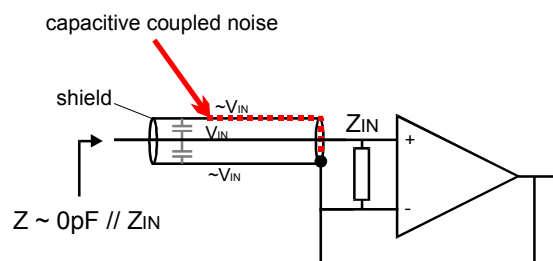


Figure C. 14. Active guarding principle.

<sup>6</sup> In the case that the shields are connected to ground, the interferences will be reduced but the undesired effect caused by the parasitic capacitances will not be avoided, if not aggravated.

When driving capacitive loads, the operational amplifier must be carefully selected to avoid instability. It must be also noted that active guarding implies some degree of positive feedback through the shield-core capacitance. Thus, it can be advisable use gain values slightly below the unity in order to minimize instability or oscillations [24].

Another strategy to compensate the parasite capacitances of the wires is to create *negative capacitances*. That is, by using negative and positive feedback circuits it is possible to implement Negative Impedance Converters (NIC's) that compensate the *positive impedances* seen by the instrumentation [25;26].

In the framework of this thesis work, the use of short unshielded wires has been often preferred as simple solution since low measurement frequencies were used ( $< 100$  kHz) and time consuming filtering was possible to reject coupled noise.

### **Front-end concept**

As an alternative or complementary strategy to active guarding it is possible to move part of the electronics to the vicinity of the electrodes. The idea is that a tiny front-end module (the module containing the circuitry close to the electrodes) is able to provide the signals to the main instrument in such a way that a comfortable separation distance is allowed without causing significant distortion.

The complexity of the front-end module can range from simple buffers or current sources [27] to complete signal conditioning [28].

### **Multiplexing**

When performing bioimpedance measurements, it can be interesting or even necessary to have multiple measurement channels available. These channels can be necessary to measure impedance from different electrode arrangements, for instance, in Electrical Impedance Tomography, or can be employed for automatic calibration.

Unfortunately, apart from the evident fact that multiplexing will decrease the sampling rate per channel, the switching mechanism can imply some drawbacks that result in a reduction of the overall performance. Among those drawbacks, probably, the parasitic capacitances and resistances of the switches are the most significant ones.

Currently, the most common switching mechanisms for analogue signals are based on analog integrated switches and relays. The following table summarizes their advantages and disadvantages.

**Table C. 1.** Comparison between solid state switching and relays.

	Advantages	Disadvantages
<b>Analogue integrated switches</b>	<ul style="list-style-type: none"> <li>▪ Low power consumption</li> <li>▪ Simplified control</li> </ul>	<ul style="list-style-type: none"> <li>▪ Cross-talking (annoying at frequencies &gt;100 kHz)</li> <li>▪ High input parasitic capacitances.</li> </ul>
<b>Relays</b>	<ul style="list-style-type: none"> <li>▪ Excellent isolation and conductance</li> </ul>	<ul style="list-style-type: none"> <li>▪ Moderate size an weight</li> <li>▪ Slow response</li> <li>▪ Limited life</li> </ul>

It must be taken into account that the influence of the parasitic elements can be minimized in the case that a each channel has its own front-end electronics before the switching mechanism [29].

## Noise

When dealing with low level signals it is always advisable to implement analog electronic designs with low intrinsic noise features [10]. However, taken into account that the signals involved in bioimpedance measurements will be generally above 1 Hz, that narrow bandwidths will be selected (<10 Hz) and that ultra-high resolution is not required (< 14 bits), the intrinsic noise troubleshooting can almost be ignored in favor of external noise and interference generators which are more annoying. Those sources are:

- Electrical noise and interferences generated by the sample. As any conductor, the sample will generate some electrical noise due to the Johnson effect. What is more important, in some cases, such as the beating heart, there will be interference signals generated by the sample itself (action potentials). Those effects will be minimized by selecting a proper measurement frequency and a narrow bandwidth.
- Motion artifacts. Their disastrous effect will last for a period longer that the temporary disconnection of an electrode since quiescent point will have to be reached again.
- Environmental interference signals. The insidious 50 Hz or 60 Hz interference from the mains supply will enter into the signal path through the electro leads. Measures against capacitive coupled noise (i.e. shielding) are highly advisable.
- Noise and interferences generated by the other parts of the instrumentation system. In order to minimize interferences from the digital circuitry, it is advisable to use separate ground planes and supply lines. It is also advisable to avoid switched regulators and switched power supplies since those elements work at frequencies (typically form 10 kHz to 100 kHz) that can be within the bandwidth of interest.



## **C.2. Developed systems**

Here are presented some of the bioimpedance systems that have been developed in the framework of this thesis. The first three ones have been employed to obtain the experimental results that are described across the thesis report. The others have been included as examples of the concepts introduced above.

Other instruments also related to bioimpedance measurements and to the MicroTrans and MicroCard projects are not described here. Among them, it must be mentioned the measurement systems based on PDAs (for Personal Digital Assistant) [30;31]

### C.2.1. Analog multi-frequency and multi-channel bioimpedance meter for low frequencies (< 100 kHz)

During the first stages of the MicroTrans project, it was necessary to develop a portable instrument for recording bioimpedance at 1 kHz from multiple channels. This instrument ought to be compatible with other instruments also connected to the sample (pH, K<sup>+</sup> and temperature sensors). Taken that into account, a set of modules with analog outputs and digital control was developed to implement a complete virtual instrumentation system based on an acquisition board. The overall architecture is briefly described below:

The system nucleus is a PC computer that includes a 16 bits ADC board (CIO-DAS802/16 from ComputerBoards, Inc). It powers and controls all the measurement modules that communicate the measured values through analog signals.

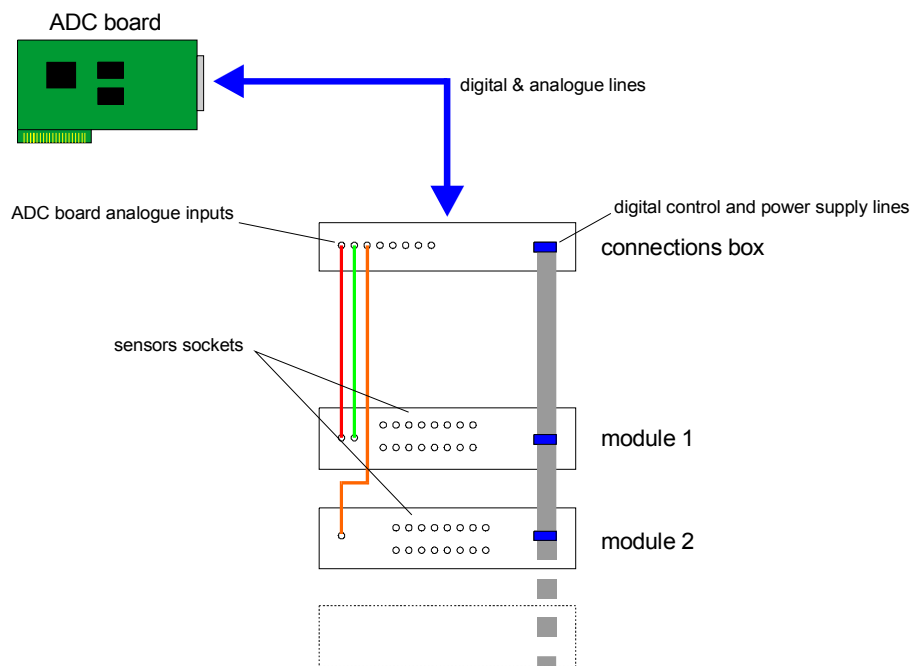
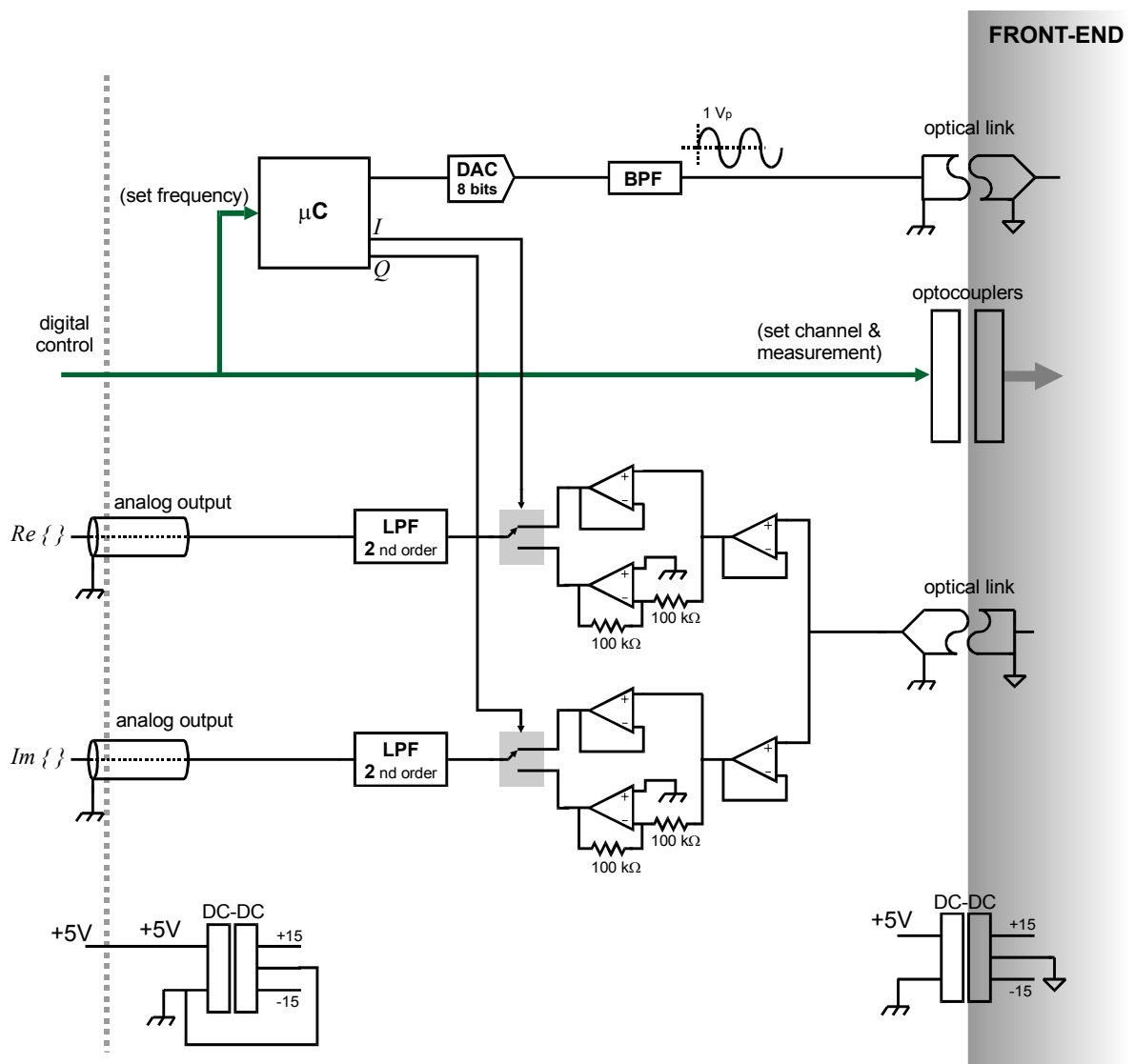


Figure C. 15. Measurement system architecture.

Since high frequency signals are not involved, LabVIEW™ is a good software platform to develop the required software modules to control, to process, to display and to store the measured data provided by the ADC board. The software controls the analog multiplexers in each measurement module and reads the value associated with the measure from one specific channel, then, after performing some mathematical processes (scaling, offset compensation, filtering...) the value is stored in the hard disk and displayed in a time evolving graph on the computer screen.

The bioimpedance module implementation has evolved significantly over the MicroTrans project. For instance, at the beginning, the fixed frequency sine generation was performed by an IC based on a sine converter (XR-8038) whereas now it is possible to select one of eight frequencies that are generated by a microcontroller. Only the current version is described here.

The module has been implemented according to Figure C. 1. That is, it is composed of two parts: an electrically isolated signal conditioning sub-system and a gain/phase analyzer. In fact, each sub-system has been implemented in a Printed Circuit Board (PCB). The signal conditioner is completely equivalent to the front-end module described in the next section. The main parts of the gain/phase analyzer are shown in Figure C. 16.



**Figure C. 16.** Schematic diagram of the gain/phase analyzer embedded into the bioimpedance module.

According to the frequency ordered by the computer, the microcontroller ( $\mu\text{C}$ ) generates a stream of digital values that is converted by the digital-to-analog converter (DAC) into a sinusoidal signal. The microcontroller also generates two digital signals, I and Q, that are respectively in phase and in quadrature (signal delayed  $T/4$ ) with respect to the sin signal. Those signals control the switch of the demodulators based on sign switching in such a way that the outputs provide the real and the imaginary parts of the signal supplied by the front-end. As it is described in the next section, that signal from the front-end can represent the voltage drop or the current flowing through the sample, the computer is responsible for selecting the sort of measurement.

From the real and imaginary parts of the current and the voltage, the virtual instrument running on the PC computes the impedance magnitude and phase values.

The features of the overall system are similar to those presented in the next section. However, it must be mentioned that beyond 100 kHz the design of the demodulator based on sign switching requires high speed operational amplifiers and analog switches. Another important drawback of this structure is that the demodulators are shared by all the channels for the voltage and current signals and that implies long wait times to avoid cross interference.

### C.2.2. Multi-channel optically isolated front-end

This module is intended to work with any gain/phase analyzer connected to a computer in order to implement a bioimpedance measuring system based on the four-electrode method. Its main features are:

- digitally controlled.
- 10 measuring channels.
- electrical ground isolation.
- Bandwidth: 100 Hz to 100 kHz

The complete system architecture is similar to that shown in Figure C. 1. As an extra feature, the front-end module can also provide the V- signal which is almost directly related to common voltage. Such reading can be used to study the evolution of the tissue-electrode interface impedance while four electrode measurements are being performed.

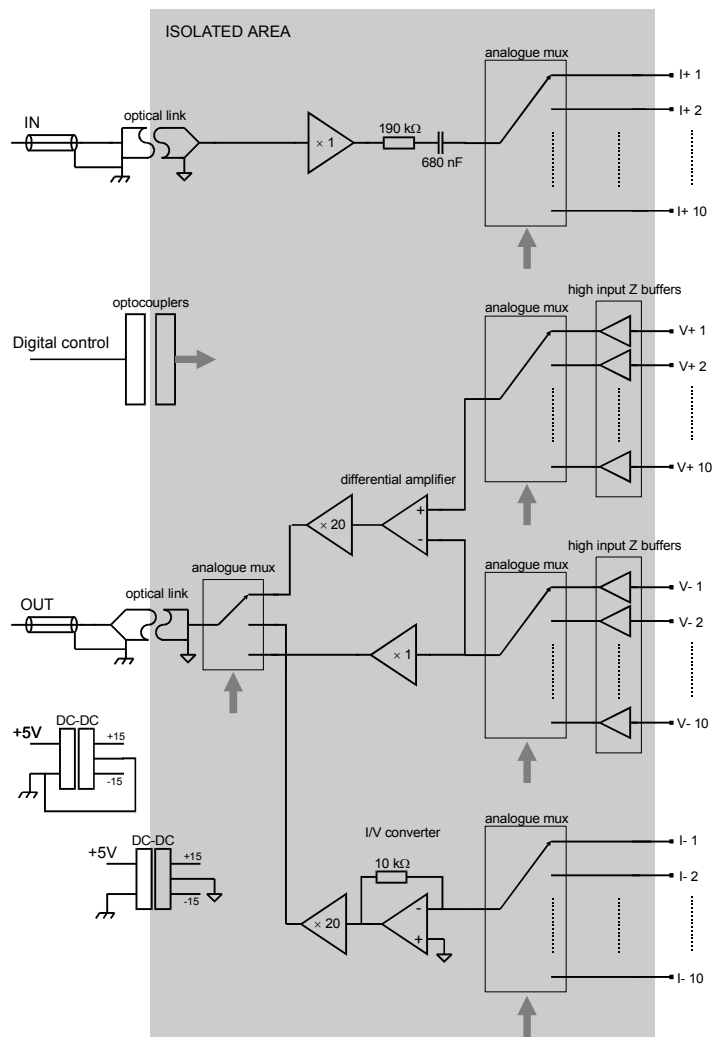


Figure C. 17. Impedance front-end blocks diagram.

The front-end module receives and transmits voltage and current signals through analogue optical links in order to have electrical isolation from ground. A single output link is used to send voltage and current signals (time multiplexed) to the gain-phase analyzer and an input link is used to receive the voltage signal from the voltage oscillator included in the gain-phase analyzer.

These optical links show linearity and high frequency bandwidth but they introduce gain-phase errors. It is possible to minimize these errors by adjusting trimmers during the adjustment stages but, even in this case, errors will be manifested during the system usage due to temperature changes and ageing. Therefore, an automatic error compensation (calibration) method is strongly recommended. A well known impedance such a resistor in one of the channels can be used to determine the transfer function values (magnitude and phase) at each frequency of interest.

**Table C. 2. Some crucial parts of the front-end module**

Description	Part
OA used as voltage followers for buffering	AD713J/AD
16 channel analog multiplexer	DG406
DC-DC converter	NMXD0515SO (Newport)
Analog optical link	HCPL-4562 (Agilent)
Differential amplifier	AD830
Output analog multiplexer	DG303A
Other OAs	TLE2037CP

**Table C. 3. Features experimentally verified**

Parameter	Value
CMRR	@ 1 kHz 88 dB
	@ 10 kHz 88 dB
	@100 kHz 66 dB
input common impedance	>50 M $\Omega$ // 7pF
input differential impedance	>50 M $\Omega$ // 2pF
Ground isolation impedance	~ 50 pF

This front-end module has been successfully employed by the AMCA team in conjunction with lock-in Amplifier 7220 from Signal Recovery (AMETEK, Inc.)

### C.2.3. Simple front-end for Solartron 1260

The 1260A Impedance Analyzer (Solartron Analytical, [www.solartronanalytical.com](http://www.solartronanalytical.com)) is an excellent instrument for a broad range of impedance applications. It is able to perform four-electrode measurements but, unfortunately, its input impedance at the  $V+$  and  $V-$  terminals ( $1\text{ M}\Omega // 35\text{ pF}$  according to its specifications) can be too low for those applications in which the electrode impedances are high such as in the case of bioimpedance measurements at low frequencies. Moreover, the CMRR does not seem to be the best achievable ( $>50\text{ dB}$  at  $1\text{ MHz}$  according to specifications). Those issues motivated the implementation of a very simple front-end for bioimpedance measurements at low frequencies ( $< 100\text{ kHz}$ ).

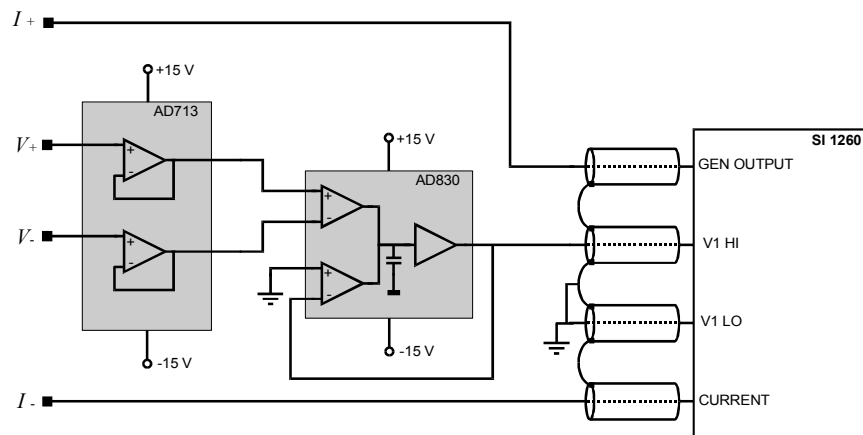


Figure C. 18. Simple front-end for Solartron 1260.

A one-of-four multiplexer based on relays (G6A-434P 4PCO, Omron Corp.) was also developed in order to be able to record simultaneously the impedance from up to four impedance probes. The overall system architecture is shown in Figure C. 19.

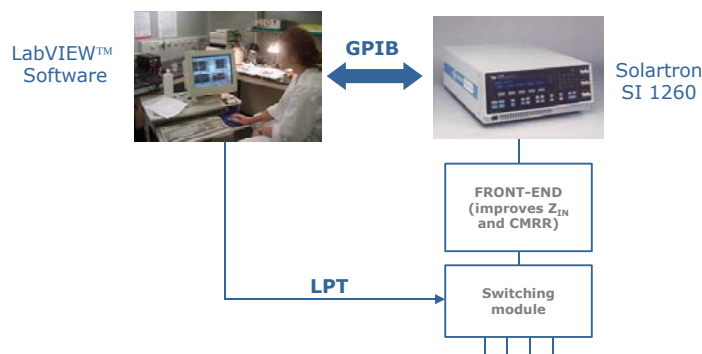


Figure C. 19. Architecture of the system based on the 1260 Impedance Analyzer.

It must be noted that between the front-end and the impedance probes, including the multiplexer, the signal lines were not shielded and none method for capacitive coupling avoidance was provided. Therefore, these connections and wires were made as short as possible.

### C.2.4. Single frequency bioimpedance logger

This complete bioimpedance meter was implemented<sup>7</sup> for pneumography in diving [32]. It registers the trans-thoracic impedance values at 100 kHz and stores them in an internal non-volatile memory for up to two hours.

Figure C. 20 shows the main parts of this device. The microcontroller ( $\mu\text{C}$ ) generates a clock signal of 400 kHz (not shown) for the Programmable Logic Device (PLD). From this signal, the PLD generates a 100 kHz rectangular signal that, after being filtered, is injected to the subject through a 100 k $\Omega$  resistor. The PLD also generates the required sampling clock signals to obtain two sets of samples: a) in perfect synchrony with the 100 kHz signal and b) in synchrony with the 100 kHz signal plus a T/4 delay (2.5  $\mu\text{s}$ ). From the digital demodulation expressions, it can be easily demonstrated that the average of the first set of samples is proportional to the real part of the impedance while the average of the second set is proportional to the imaginary part. In this way, the real part and the imaginary part are obtained, filtered and stored in the Flash memory by the microcontroller.

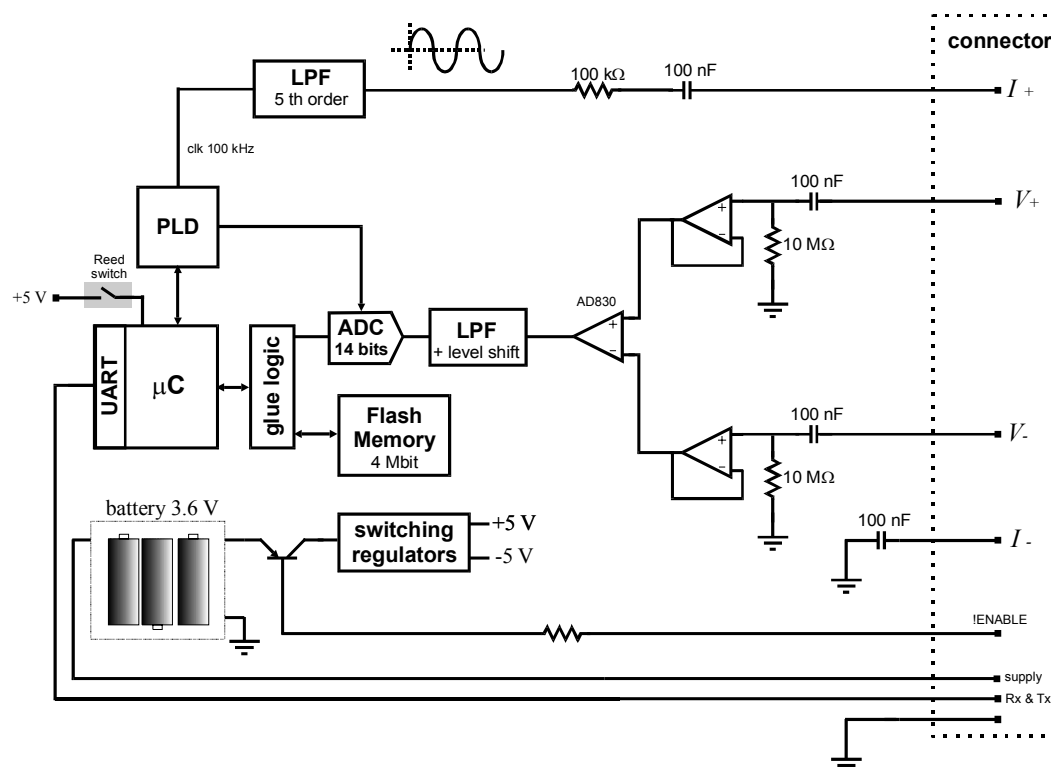


**Figure C. 20.** Schematic diagram of the bioimpedance logger. A single connector has been included to prevent simultaneous connection of the device to the subject and to the computer or the charger. The Reed switch (magnetically actuated switch) can be used to put marks in the log file.

<sup>7</sup> In this case, the system design was performed by our group but the actual implementation of the device was performed by Diprotech, S.L.



It must be noted that this device does not include a current source nor measures the current flowing through the subject. Fortunately, for the pneumography application, it can be assumed that the sample has a very low impedance ( $< 1\text{k}\Omega$ ) compared to the output resistor ( $100\text{ k}\Omega$ ) and, therefore, the current can be considered constant.

**Table C. 4.** Main features of the device.

Parameter	Value
Power supply	Internal batteries ( $3 \times 1.2\text{ V}$ )
Measurement frequency	100 kHz
Injected current	$< 100\ \mu\text{A}_p$
Measurable impedance range	$5\ \Omega$ to $100\ \Omega$
Measurement method	Four-electrode method
Electrodes	ECG electrodes (Mod. 2330, 3M Health Care)
Sampling rate	8 samples/s
Memory	4 Mbit (2 hours)

The device does not include trimmers or any other adjustment mechanisms. The compensation of offset voltages, gain errors and phase shifts is performed after downloading the data by an automatic calibration process. It is based on the measurement of a shunt to cancel offset voltages and the measurement of a well known impedance (e.g. a  $33\ \Omega$  resistor) to compensate gain errors and phase shifts.

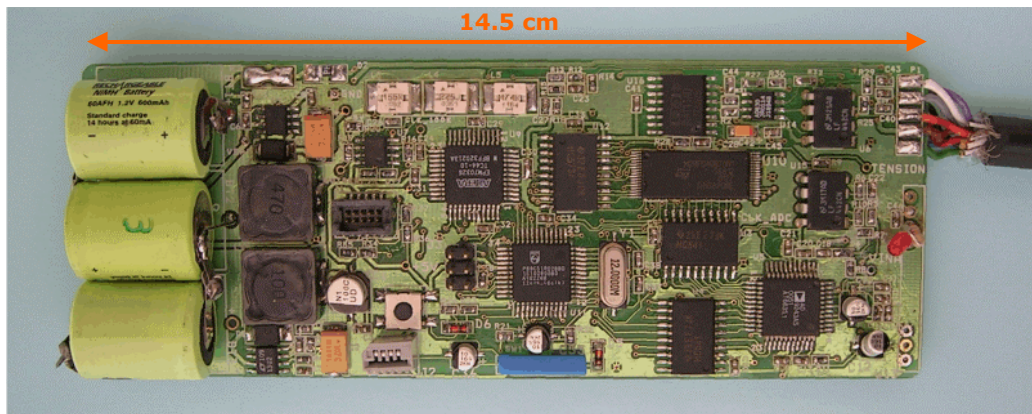


**Figure C. 21.** Picture of the bioimpedance logger taken before silicone packaging.

### C.2.5. Digital multi-frequency system

This module has been implemented<sup>8</sup> as a low cost alternative to the Solartron 1260. It does not reach the SI 1260 features concerning resolution, dynamic range and frequency span but it should be useful for a wide range of bioimpedance applications. Moreover, the chance to change some of the components (e.g. resistors that determine the gains) allows us to adapt it to the specific application.

Figure C. 22 shows the main parts of the module. The microcontroller ( $\mu\text{C}$ ) does not perform any computation at all, it simply acts as a bridge between the external computer and the module through the serial link. The commands received from the computer specify the DDS frequency (from 1 Hz to 1MHz), the gains of the Programmable Gain Amplifiers (PGA), the output resistance (limit output current to  $5\mu\text{A}_p$ ,  $50\mu\text{A}_p$  or  $0.5\text{ mA}_p$ ) and the sampling rate. The circuitry of the Programmable Logic Device (PLD) is responsible for generating the precise sampling clock from the DDS master clock. In this way, the data received by the computer (14-bits samples of the voltage and current channels at a maximum transfer rate of 2500 samples/s) corresponds to precisely known fractions of period of the generated signal and the computer is able to perform the digital demodulation process.

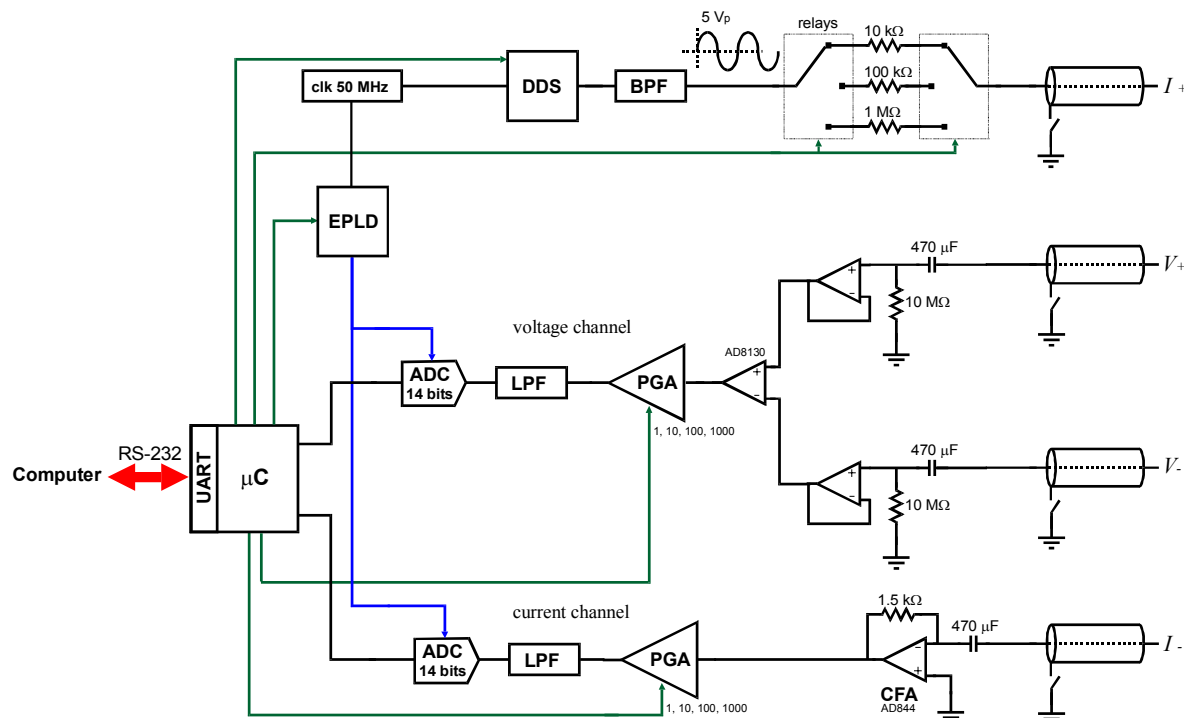


Figure C. 22. Schematic diagram of the multi-frequency bioimpedance analyzer.

<sup>8</sup> As in the previous case, the system design was performed by our group but the actual implementation was performed by Diprotech, S.L.

The module also provides power supply ( $\pm 5V$ , 200 mA) and digital control lines (TTL compatible) for complementary circuits such as front-ends or switching matrixes<sup>9</sup>.

It must be noted that the number of available samples to perform the demodulation is not limited by the sampling rate of the ADCs but because of the limited transfer rate through the serial link and the processing capabilities of the computer. This is a serious drawback concerning the measurement rate since longer acquisition periods (integration time) will be necessary for noise suppression. To improve that, it could be possible to use faster transfer links such as USB or embed the digital demodulation process within the module by employing Digital Signal Processors [11].

**Table C. 5.** Main features of the digital multi-frequency system.

Parameter	Value
Power supply	Mains supply (220 V, 50 Hz)
Galvanic isolation	None
Communications	RS-232, 115200 bps
Frequency range	1 Hz to 1 MHz <sup>*1</sup>
Frequency resolution	11.64 mHz
Measurable impedance range	10 $\Omega$ to 100 k $\Omega$ <sup>*2</sup>
Output impedance	10 k $\Omega$ , 100 k $\Omega$ or 1 M $\Omega$
Accuracy	error $ Z  < 0.1$ % FS error $\angle Z < 0.1$ degrees <sup>*3</sup>
CMRR	@ DC - 100 kHz > 100 dB <sup>*4</sup> @ 100 kHz - 1 MHz > 90 dB
V+ and V- input impedance	> 10 <sup>12</sup> $\Omega$ // 10pF <sup>*5</sup>

<sup>\*1</sup> In the case that the protection capacitances are shunted it is even possible to work at frequencies lower than 0.1 Hz

<sup>\*2</sup> Can be expanded by changing some internal resistances.

<sup>\*3</sup> These illustrative figures have been obtained for 5 k $\Omega$  impedances at frequencies below 100 kHz. The integration time was 1 second.

<sup>\*4</sup> Experimentally verified

<sup>\*5</sup> Only in the case that the protection input capacitances and the 10 M $\Omega$  polarization resistances are suppressed. It has been verified that the input capacitance can be neglected without causing noticeable problems.

<sup>9</sup> A one-of-eight multiplexer based on relays has also been implemented. It is not only intended for multiple channel measurements but also for on-line calibration purposes.

## References

1. Okada, K. and Sekino, T., *The impedance Measurement Handbook, a guide to measurement technology and techniques* Agilent Technology Co. Ltd., 2003.
2. Morucci, J.-P., Valentinuzzi, M. E., Rigaud, B., Felice, C. J., Chauveau, N., and Marsili, P.-M., "Bioelectrical Impedance Techniques in Medicine," *Critical Reviews in Biomedical Engineering*, vol. 24, no. 4-6, pp. 223-681, 1996.
3. Geddes, L. A. and Baker, L. E., "Detection of Physiological Events by Impedance," in Geddes, L. A. and Baker, L. E. (eds.) *Principles of applied biomedical instrumentation* Third Edition ed. New York: Wiley-Interscience, 1989, pp. 537-651.
4. Franco, S., "Signal generators," *Design with operational amplifiers and analog integrated circuits* New York: McGraw-Hill, 1988, pp. 354-409.
5. Riu, J. P., Elvira, J., Oliver, M. A., Gobantes, I., and Arnau, J. In-situ assessment of the technical quality of meat. 619-622. 2001. Oslo, Norway. XI International Conference on Electrical Bio-Impedance. 17-6-2001.  
Ref Type: Conference Proceeding
6. Shróder, J., Doerner, S., Schneider, T., and Hauptmann, P., "Analogue and digital sensor interfaces for impedance spectroscopy," *Measurement Science and Technology*, vol. 15 pp. 1271-1278, 2004.
7. Oppenheim, A. V., Willsky, A. S., and Young, I. T., *Signals and systems* London: Prentice-Hall International, 1983.
8. Carlson, A. B., *Communication systems: introduction to signals and noise in electrical communication* New York: McGraw-Hill Education, 1986.
9. Pallás-Areny, R. and Webster, J. G., "Bioelectric impedance measurements using synchronous sampling," *IEEE Transactions on Biomedical Engineering*, vol. 40, no. 8, pp. 824-829, Aug.1993.
10. Pallás-Areny, R. and Webster, J. G., *Sensors and signal conditioning*, 2nd ed. New York: John Wiley & Sons Inc, 2001.
11. Dudykevych, T., Gersing, E., Thiel, F., and Hellige, G., "Impedance analyser module for EIT and spectroscopy using undersampling," *Physiological Measurement*, vol. 22 pp. 19-24, 2001.
12. Kester, W., "Undersampling applications," Norwood MA, USA: Analog Devices, 1995, pp. 5.1-5.33.
13. Kinouchi, Y., Iritani, T., Morimoto, T., and Ohyama, S., "Fast in vivo measurements of local tissue impedances using needle electrodes," *Med.Biol.Eng.Comput.*, vol. 35 pp. 486-492, 1997.
14. Harms, J., Schneider, A., Baumgartner, M., Henke, J., and Busch, R., "Diagnosing acute liver graft rejection: experimental application of an implantable telemetric impedance device in native and transplanted porcine livers," *Biosensors & Bioelectronics*, vol. 16 pp. 169-177, 2001.
15. Pliquett, U. Fast impedance measurements and non-linear behaviour. 2, 739-742. 2004. Gdansk, Poland. Proceedings of the XII International Conference on Electrical Bioimpedance (ICEBI).  
Ref Type: Conference Proceeding

16. Casas, O, "Contribución a la obtención de imágenes paramétricas en tomografía de impedancia eléctrica para la caracterización de tejidos biológicos." PhD Thesis Universitat Politècnica de Catalunya, 1998.
17. Nebuya, S., Noshiro, M., Brown, B. H., Smallwood, R. H., and Milnes, P., "Accuracy of an optically isolated tetra-polar impedance measurement system," *Med.Biol.Eng.Comput.*, vol. 40 pp. 647-649, 2002.
18. Cook, R. D., Saulnier, G. J., Gisser, D. G., Goble, J. C., Newell, J. C., and Isaacson, D., "ACT3: a high-speed, high-precision electrical impedance tomograph," *IEEE Transactions on Biomedical Engineering*, vol. 41, no. 8, pp. 713-722, Aug.1994.
19. Yélamos, D., Casas, O., Bragos, R., and Rosell, J., "Improvement of a front end for bioimpedance spectroscopy," *Annals of the New York Academy of Sciences*, vol. 873 pp. 306-312, 1999.
20. Hoyle, C. and Peyton, A. Bootstrapping techniques to improve the bandwidth of transimpedance amplifiers. 7-1-7/6. 1998. Oxford UK. IEE Colloquium on Analog Signal Processing. 28-11-1998.  
Ref Type: Conference Proceeding
21. Bragos, R., Blanes, P., Riu, P. J., and Rosell, J. Comparison of current measurement structures in voltage-driven tomographic systems. 8-1-8/3. 1995. London. IEE Colloquium on Innovations in Instrumentation for Electrical Tomography. 11-5-1995.  
Ref Type: Conference Proceeding
22. Pallás-Areny, R. and Webster, J. G., "AC instrumentation amplifier for bioimpedance measurements," *IEEE Transactions on Biomedical Engineering*, vol. 40, no. 8, pp. 830-833, Aug.1993.
23. Ghahary, A. and Webster, J. G. Electrical safety for an electrical impedance tomograph. 2, 461-462. 1989. Seattle, WA USA. Proceedings of the XI Annual International Conference of the IEEE Engineering in Medicine and Biology Society. 9-11-0004.  
Ref Type: Conference Proceeding
24. Goovaerts, H. G., Faes, T. J. C., Raaijmakers, E., and Heetharr, R. M., "A wideband high common mode rejection ratio amplifier and phase-locked loop demodulator for multifrequency impedance measurement," *Med.Biol.Eng.Comput.*, vol. 36 pp. 761-767, 1998.
25. Soundararajan, K. and Ramakrishna, K., "Nonideal negative resistors and capacitors using an operational amplifier," *IEEE Transactions on Circuits and Systems*, vol. 22, no. 9, pp. 760-763, 1975.
26. Bertemes-Filho, P., Lima, R. G., and Amato, M. B. P. Capacitive-compensated current source used in electrical impedance tomography. 2, 645-648. 2004. Gdansk, Poland. Proceedings of the XII International Conference on Electrical Bioimpedance. 20-6-2004.  
Ref Type: Conference Proceeding
27. Jossinet, J., Tourtel, C., and Jarry, R., "Active current electrodes for in vivo electrical impedance tomography," *Physiological Measurement*, vol. 15 pp. A83-A90, 1994.
28. Bragos, R., Ramos, J., Salazar, Y., Fontova, A., Fernández, M., Riu, J. P., García-Gonzalez, M. A., Bayés-Genís, A., Cinca, J., and Rosell, J. Endocardial impedance spectroscopy system using a transcatheter method. 465-468. 2004. Gdansk, Poland. Proceedings from the XII International Conference on Electrical BioImpedance (ICEBI). 20-6-0004.  
Ref Type: Conference Proceeding

29. Ramos, J., Pallás-Areny, R., and Tresànceh, M., "Multichannel front-end for low level instrumentation signals," *Measurement*, vol. 25 pp. 41-46, 1999.
30. Ivorra, A., Corredera, A., and Aguiló, J. PDAs y Bluetooth: dos nuevas herramientas para la construcción de instrumentación biomédica. 261-264. 27-11-2002. Zaragoza, Spain. XX Congreso Anual de la Sociedad Española de Ingeniería Biomédica. 27-11-2002.  
Ref Type: Conference Proceeding
31. Villa, R., Sánchez, L., Guimerà, A., Ivorra, A., Gómez, C., and Aguiló, J. A new system for the bioimpedance monitoring of organs for transplattation. 119-122. 2004. Gdansk, Poland. Proceedings from the XII International Conference on Electrical Bio-Impedance. 20-6-0004.  
Ref Type: Conference Proceeding
32. Dalmases, M., Ivorra, A., Villa, R., Blanch, L., Villagrà, A., López, J., Piacentini, E., and Desola, J. Electrical impedance monitoring: preliminary results on risk detection of Intrathoracic Hyperpressive Syndrome in diving. 103-106. 2004. Gdansk, Poland. Proceedings from the XII International Conference on Electrical Bio-Impedance (ICEBI). 20-6-0004.  
Ref Type: Conference Proceeding



